24th INTERNATIONAL CONGRESS ON SOUND AND VIBRATION
23–27 July 2017, London

ANALYSIS OF THE DYNAMICS OF THE FLYWHEEL WITH NONLINEAR VIBRATION ABSORBER USING WAVELETS

Liu Haiping

Beijing Institute of Spacecraft System Engineering, Beijing 100094, China.
email: lhpvibration@163.com.cn

Wang Yaobing

Beijing Institute of Spacecraft System Engineering, Beijing 100094, China.

Sun Pengfei

Beijing Institute of Spacecraft System Engineering, Beijing 100094, China.

Xu Zhe

Beijing Institute of Spacecraft System Engineering, Beijing 100094, China.

The micro-vibration from the flywheel system (such as, momentum wheel and reaction wheel), as the one of main disturbances, has restricted the effective use of high sensitive payloads in the satellites. In order to suppress the low-frequency line spectrum from the flywheel, the nonlinear vibration absorber (NVA) using Euler buckled beam is developed. A discrete multi-degree-of-freedom dynamic model, which includes the NVA, the flywheel and the supporting structure, is built. The NVA is represented by a linear positive stiffness spring and Euler buckled beams in parallel. Based on the nonlinear dynamic equations, the systematic dynamic equations without and with the NVA are solved by using Four-order Runge-Kutta Method under the micro-vibration from the flywheel in time-domain. Considering the energy pumping phenomenon of the NVA can be excited when the input energy satisfies a specific threshold, the wavelet transform is used to deal with the calculating data from the dynamic model in order to analyse the response performance of the NVA and the controlled object. Compared with the vibration responses of the controlled object without and with the NVA, it can be concluded that the NVA exhibits high performance in energy transfer and dissipation where the responses are strongly dominated by 1:1 resonance capture. Meanwhile, the apparent unsteady time-vary signals can be found with varying of the input energy.
Keywords: flywheel, nonlinear vibration absorber, NVA, wavelets

1. Introduction

The vibration from flywheel and control momentum gyroscopes, as the one of main disturbances, has restricted the effective use of high sensitive payloads in the satellite [1-4]. There would be large dynamic amplification when the rotational speed of the flywheel intersects with the natural frequencies, which is considered due to gyroscopic effect. This phenomena leads to some low-frequency line spectrum disturbances, which cannot be isolated effectively due to the frequencies of the disturbances close to the transition frequency of the isolating system [5].

Comparing with the linear vibration absorber, the nonlinear vibration absorber (NVA) exhibits some merits, such as absorbing vibrations over a broadband, high efficiency in vibration control, relatively small mass, and without the need for additional energy [6,7]. The design frequency of vibration control devices in spacecraft need relatively broad spectrum due to strict restriction in the field of payloads' weight, energy consumption, and complicated cases in the stages of launching and working in the orbit.

In order to control the disturbances from the flywheel in the stage of working in the orbit, a nonlinear vibration absorber with an Euler buckled beam, which paralleled with a linear spring, is exhibited in this paper. According to the practical application, a discrete multi-degree-freedom dynamic model, which represent the flywheel, the NVA and the supporting structure system, is addressed. Using the established models, a computer simulation is carried out to investigate the apparatus's performance under transient responses by using Runge-Kutta method. To study the frequency contents of the calculating results and research energy transition among components from this nonlinear dynamic system, the Morlet wavelet transform method is applied to the relative responses. Finally, some concluding remarks with important features of this work are conducted.

2. Dynamic modelling of the nonlinear vibration absorber (NVA)

The NVA is built by using four Euler buckled beams and a linear spring, as shown in Figure 1. In this model, the influence from the weight of the lumped mass has been cancelled due to the supporting stiffness from the linear spring.

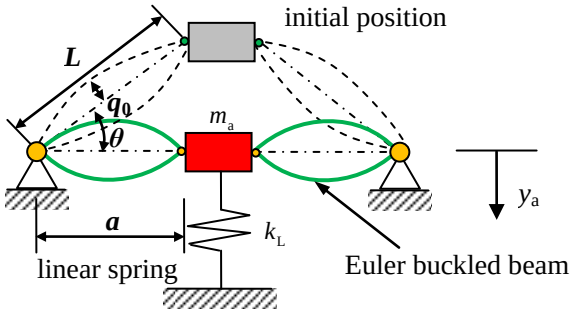

Figure 1: Schematic of the nonlinear vibration absorber model.

In the initial phase, a single Euler beam subjects to constant vertical loading P, as shown in Figure 2. q_0 represents the initial imperfection at the centre of the Euler beam, y and q represents the axial deflection of the beam and the imperfection under the axially force P, respectively.

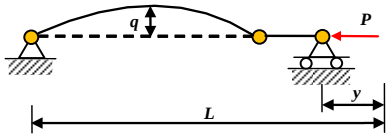

Figure 2: Schematic of a single Euler beam model.

The relationship between the axially force P and the end displacement y:

$$P = P_e\left[1-\pi\left(\frac{q_0}{L}\right)\left(\pi^2\left(\frac{q_0}{L}\right)^2+4\left(\frac{y}{L}\right)\right)^{-1/2}\right]\left[1+\frac{\pi^2}{8}\left(\frac{q_0}{L}\right)^2+\frac{1}{2}\left(\frac{y}{L}\right)\right] \tag{1}$$

where $P_e=EI(\pi/L)^2$ is the Euler critical load, L is initial length of the Euler beam, E is the material Young's modulus, I is the area moment of inertia for square cross-sectional area of the Euler beam.

The horizontal position of the lumped mass is assumed to be the equilibrium state. The relationship between force and displacement of the NVA can be acquired:

$$F = k_L k_1' L\frac{y_a}{L}+k_L k_3' L\left(\frac{y_a}{L}\right)^3+k_L L\sqrt{1-\gamma^2}-m_a g \tag{2}$$

where, F represents the restoring force, k_L represents the linear spring stiffness, h represents the sectional height of the Euler beam, w represents the sectional width of the Euler beam, $\gamma=\cos\theta=a/L$, $I = wh_a^3/12$, $k_1=[(a-b)/a\gamma](b^2/2-2\gamma+6)$, $k_3=(a-b)/a\gamma+[(a-b)/2\gamma^3a+b/\gamma^2a^3](b^2/2-2\gamma+6)$, $k_1' = 1-\lambda k_1$, $k_3' = \lambda k_3$, $b=\pi q_0/L$ and $\lambda=P_e/k_LL$, $k_L L\sqrt{1-\gamma^2} = m_a g$ 。

3. Dynamic modelling of the flywheel-NVA-supporting structure

The systematic dynamic model of the flywheel-NVA-supporting structure is proposed, as presented in Figure 3. As shown in Figure 3, M_m and k_m is the mass and stiffness of the supporting structure, c_m is the supporting structure's damping coefficient; m_a and c_a is the mass and damping coefficient of the NVA, respectively; $F(z)$ is the restoring force and f_t is the disturbance from the flywheel.

Practically, the flywheel is fixed on the aluminum honeycomb sandwich plate. The flywheel is simplified by an equivalent lumped mass M_t, stiffness element k_r and damping coefficient c_r, and the aluminum honeycomb sandwich plate is represented by the lumped mass element M_m, stiffness element k_m and damping coefficient c_m.

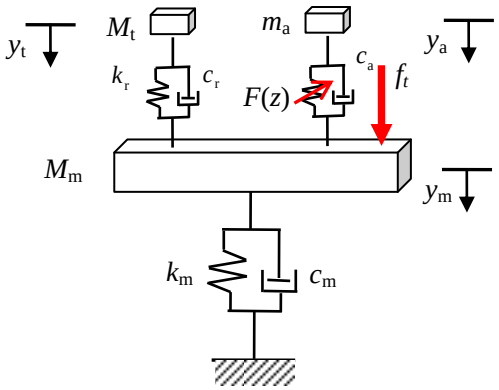

Figure 3: Schematic of the flywheel-NVA-supporting structure model.

The equations of the systematic motion can be written as follows:

$$\begin{cases} M_m\ddot{y}_m + c_m\dot{y}_m + k_m y_m + c_a\left(\dot{y}_m - \dot{y}_a\right) + k_L L\left[k_1'\dfrac{y_m - y_a}{L} + k_3'\left(\dfrac{y_m - y_a}{L}\right)^3 + \sqrt{1-\gamma^2}\right] - m_a g \\ +k_r\left(y_m - y_t\right) + c_r\left(\dot{y}_m - \dot{y}_t\right) = f_t \\ m_a\ddot{y}_a + c_a\left(\dot{y}_a - \dot{y}_m\right) + k_L L\left[k_1'\dfrac{y_a - y_m}{L} + k_3'\left(\dfrac{y_a - y_m}{L}\right)^3 + \sqrt{1-\gamma^3}\right] - m_a g = 0 \\ M_t\ddot{y}_t + k_r\left(y_t - y_m\right) + c_r\left(\dot{y}_t - \dot{y}_m\right) = 0 \end{cases} \tag{3}$$

The effectiveness of the NVA is examined in terms of vibrational energy. The transient response of the supporting structure is induced by impulsive forcing, giving the initial conditions equal to $y_m(0) = y_t(0) = y_a(0) = 0$, $\dot{y}_t(0) = \dot{y}_a(0) = 0$, $\dot{y}_m(0) \neq 0$.

The initial energy of the system is stored in the supporting structure given by:

$$E_{int} = \frac{M_m\dot{y}_m(0)^2}{2} \tag{4}$$

The total energy at time t within the flywheel is exhibited as the sum of the potential and kinetic energies:

$$E_t(t) = \frac{M_t\dot{y}_t(t)^2}{2} + \frac{k_t(y_t(t) - y_m(t))^2}{2} \tag{5}$$

The stored energy within the NVA can be found:

$$E_a(t)=\frac{m_a\dot{y}_a(t)^2}{2}+\frac{k_L k_1' L(y_a(t)-y_m(t))^2}{2}+\frac{k_L k_3' L(y_a(t)-y_m(t))^4}{4} \tag{6}$$

The energy within the supporting structure in terms of the sum of the potential and kinetic energies:

$$E_m(t)=\frac{M_m\dot{y}_m(t)^2}{2}+\frac{k_m y_m(t)^2}{2} \tag{7}$$

To measure the performance of the NVA, the percentage of the instantaneous energy stored within the NVA is defined:

$$D_a(t)=\frac{E_a(t)}{E_m(t)+E_t(t)+E_a(t)}\times 100 \tag{9}$$

Another quantitative measure of the NVA's performance is acquired by computing the percentage of the dissipated energy:

$$D_{c_a}(t)=[\frac{c_a}{E_{\text{int}}}\int_0^T(\dot{y}_a(t)-\dot{y}_m(t))^2dt]\times 100 \tag{10}$$

4. Simulating results and discussions

The parameters of the flywheel are selected according to a typical flywheel. The mass M_t is 5.9kg, the lateral stiffness k_r is 5.24×10^6N/m and the damping coefficient c_r is 10Ns/m. The mass of the supporting structure M_m is 10kg, its supporting stiffness is $k_m=1\times10^7$N/m, its damping coefficient is c_m=50Ns/m. The nonlinear stiffness element of the NVA is made of steel with Young's modulus E=210Gpa, the sectional height h and width w of the Euler beam is 1×10^{-4}m and 1×10^{-3}m, respectively. The initial imperfection and the oblique angle of the Euler beam is fixed at $q_0=1\times10^{-3}$m and θ=10°. The other parameters of the NVA m_a=0.1kg, $k_L=3\times10^2$N/m, c_a=1Ns/m and L=0.02m are considered to study the characteristics of the nonlinear system. The gravitational acceleration g equals to 10m/s^2.

The range of the excitation levels of $y_m(0)$=0mm～10mm are studied and the percentage of the dissipated energy through the total nonlinear vibration absorber damping is presented in Figure 4. By observing this figure, one can conclude that a well-defined critical threshold of the initial energy where the NVA performs well.

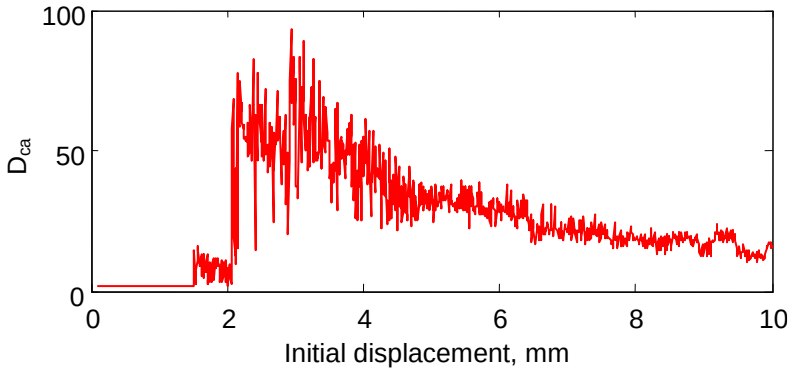

Figure 4: Percentage of the dissipated energy as a function of the initial displacement.

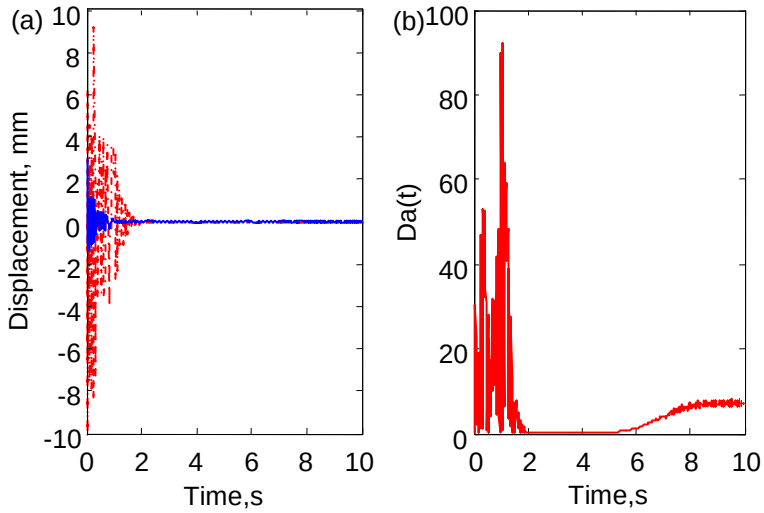

Figure 5: Simulation results for $y_m(0)$=3mm: (a) displacements y_m (solid line) and y_a (dashed line); (b) percentage of the instantaneous total energy in the NVA.

Two simulations are provided at different initial energy levels in figure 5～6. The first simulation represents a low level of the initial energy, with $y_m(0)$=3mm and E_{int}=45J. The calculating results are displayed in figure 5. It can be found that at this energy level close to the best performance of the NVA, resulting in large amplitude, and better vibration absorption. In the first time range between 0s and 1s, the NVA exhibits apparent response and the energy of the system flows into the NVA. And then, the NVA experiences dissipation slowly in the time range of 1s～2s. Finally, the energy flows back the main vibrational system again above about 2s time range.

Figure 6 illustrates the response of a simulation with a high initial energy level of $y_m(0)$=8mm and E_{int}=320J. One can found that the dramatic effects of the NVA. The system has the same overall dynamics as the previous case. Because of the increased amount of the inputting energy, the system needs a longer time to dissipate the energy.

To find the frequency contents of the above time series, a Morlet wavelet transform is applied to the displacements y_m, y_a and the relative displacement (y_a-y_m). These spectra depict the harmonic content versus time, as shown in figures 7 and 8. It can help us to study the transient variation of the harmonic components of the calculated time series. Clearly, it can be seen that the NVA performs well due to the energy from both structural modes to high frequencies at the instants.

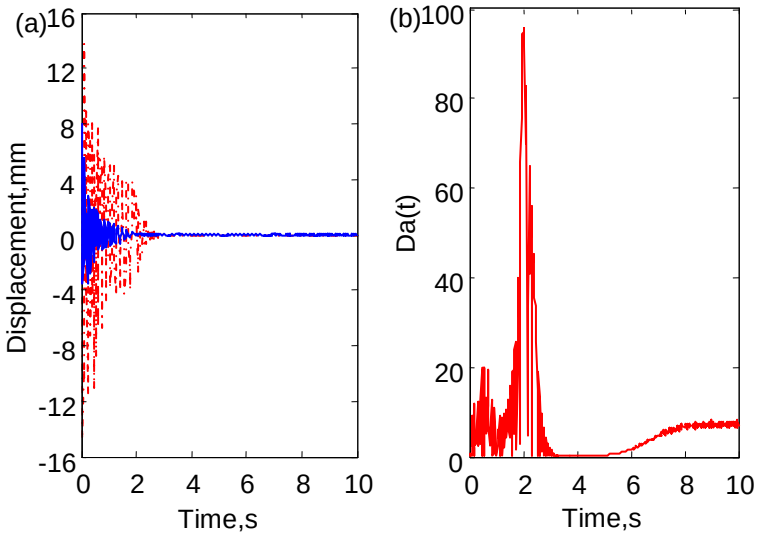

Figure 6: Simulation results for $y_m(0)$=8mm: (a) displacements y_m (solid line) and y_a (dashed line); (b) percentage of the instantaneous total energy in the NVA.

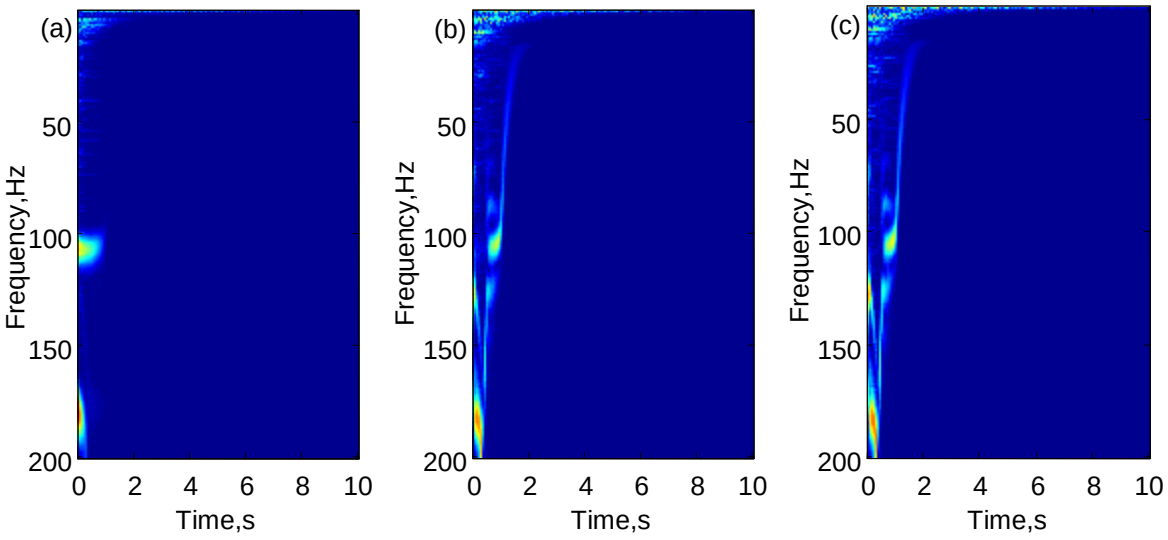

Figure 7: Wavelet spectra corresponding the time series for $y_m(0)$=3mm: (a) y_m, (b) y_a , (c) y_m-y_a.

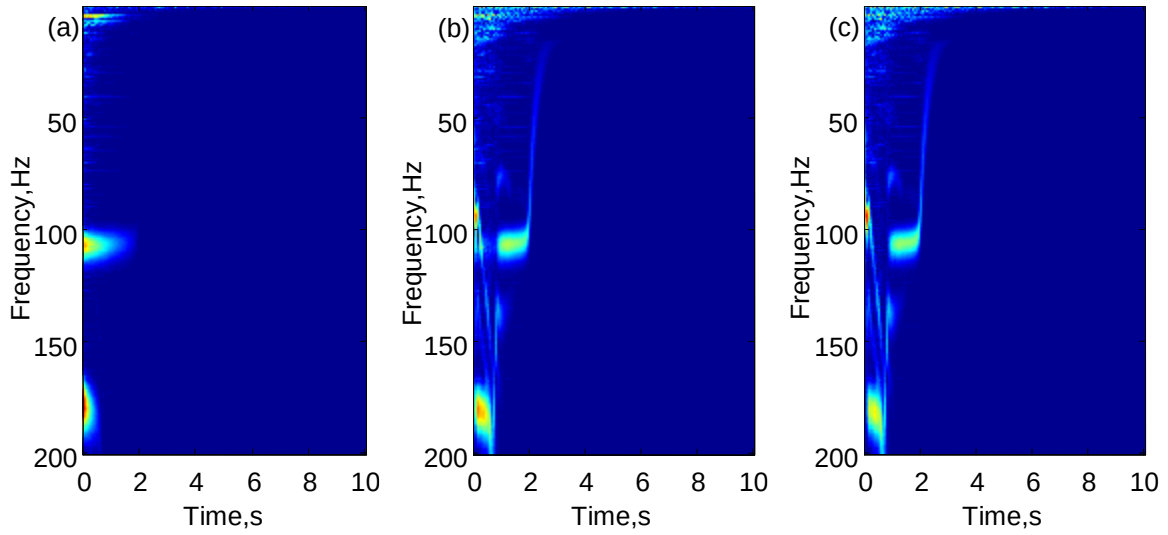

Figure 8: Wavelet spectra corresponding the time series for $y_m(0)$=8mm: (a) y_m, (b) y_a , (c) y_m-y_a.

5. Further discussion

According to the theories, the main difference between a nonlinear energy sink and a general nonlinear vibration absorber is a lack of linear stiffness. Generally speaking, a nonlinear energy sink is combined by a small mass, a cubic spring and a viscous damper. The effectiveness of the nonlinear energy sink is attributed to the nonlinear energy pumping, which corresponds to a controlled one-way channelling of the vibrational energy to a passive nonlinear structure where it localized and diminishes in time due to damping dissipation. However, in practice, it is very difficult to realize a pure cubic stiffness ideal element. Under these conditions, a useful method, which can acquire a similar nonlinear energy sink, is to minimize the influences from the linear stiffness.

To determine the restoring force contributed from the linear stiffness and the cubic stiffness, the relationship between the restoring force and the displacement of the NVA is presented by using the equation 2, as shown in figure 9. The results of the force-displacement relationship with and without the linear stiffness reveal that the nature of the cubic stiffness generated by the Euler buckled beams. It can be concluded that the NVA would be cubic stiffness and close to an ideal nonlinear energy sink.

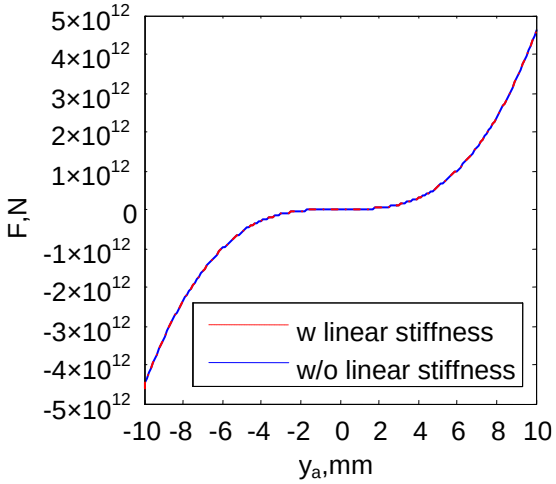

Figure 9: Relationship between force and displacement of the NVA.

6. Conclusions

For suppression the orbital vibration from the flywheel in the satellite, a nonlinear vibration absorber (NVA) is provided by using Euler buckled beams paralleled with a linear spring. Based on the boundary conditions in practice for the devices in the satellite, a discrete multi-degree-of-freedom dynamic model, which includes the NVA, the flywheel and the supporting structure, is built. Different initial displacements for the system are considered by solving the systematic equations. Furthermore, a Morlet wavelet transform is applied to the displacements in order to find the frequency contents from these time series. The results show that the NVA exhibits high performance in energy transfer and dissipation where the responses are strongly dominated by 1:1 resonance capture. And the dynamic performance of the NVA is similar to a nonlinear energy sink.

Acknowledgements

This research was supported by the National Natural Science Foundation of China (NSFC) under grant NO. 51405014.

REFERENCES

1 Meng Guang, Zhou Xu-bin. Progress review of satellite micro-vibration and control, *Acta Aeronautica ET Astronautica Sinica*, 2015, 36(8): 36-40, (2015).

2 Shao Xiao-lin. *Investigation on micro-vibration isolation technology for typical units of spacecraft*, Shanghai: Shanghai Jiao Tong University, Master Dissertation, (2013).

3 K.C. Liu, P. Maghami, C. Blaurock. Reaction wheel disturbance modeling, jitter analysis, and validation tests for solar dynamics observatory. *AIAA Guidance, Navigation and Control Conference and Exhibit*, Honolulu, (2008).

4 D.K. Kim. Micro-vibration model and parameter estimation method of a reaction wheel assemble, *Journal of Sound and Vibration*, 333: 4214-4231, (2014).

5 W.Y. Zhou, D.X. Li, Q. Luo, J. P. Jiang. Design and test of a soft suspension system for cantilevered momentum wheel assembly, *Proceedings of the Institution of Mechanical Engineers, Part G: Journal of Aerospace Engineering*, DOI: 10.1177/0954410012451415, (2012).

6 G. Kopidakis, S. Aubry, G. P. Tsironis. Targeted energy transfer through discrete breathers in nonlinear systems, *Physical Review Letters*, 87(16): 165501-1-165501-4, (2001).

7 O. Gendelman, L. I. Manevitch, A. F. Vakakis, R. M'Closkey. Energy pumping in coupled mechanical oscillators, Part I: dynamics of the underlying Hamiltonian systems, *Journal of Applied Mechanics*, 68: 34-41, (2001).